

Pyrolysis Characteristics and Kinetics of Sewage Sludge by Thermogravimetry Fourier Transform Infrared Analysis[†]

Jingai Shao,^{‡,§} Rong Yan,^{*,§} Hanping Chen,[‡] Baowen Wang,^{‡,§} Dong Ho Lee,[§] and David Tee Liang[§]

State Key Laboratory of Coal Combustion, Huazhong University of Science and Technology, Wuhan, 430074, People's Republic of China, and Institute of Environmental Science and Engineering, Nanyang Technological University, Innovation Center, Block 2, Unit 237, 18 Nanyang Drive, Singapore 637723

Received May 28, 2007. Revised Manuscript Received August 2, 2007

The characteristics and gas product properties of pyrolyzing sewage sludge were determined, aiming to utilize efficiently the waste for energy recovery. The pyrolysis of two predried sludge materials (S1 and S2) was conducted in a thermogravimetry analyzer (TGA). It was found that the pyrolysis mainly occurred at about 150–550 °C, with two and one reaction stages found respectively for S1 and S2. Using the global reaction kinetic model, the activation energy was calculated at ~ 30 kJ mol⁻¹ in the first reaction stage for all the selected heating rates, and the pre-exponential factors increased with the increasing heating rate. The kinetic parameters calculated explained well the pyrolysis characteristics observed. In the meantime, the gas products released under different pyrolysis conditions were analyzed online using Fourier transform infrared (FTIR) spectroscopy; the results showed that the gas composition was highly dependent on temperature, and the releasing of the gas species was consistent with the weight loss of sludge in pyrolysis. Thermodynamic simulation using Outokumpu HSC Chemistry version 4.1 was conducted to predict the thermodynamically predominant gas species at different temperatures. A further analysis by dividing the whole pyrolysis of sludge into 5 temperature regions revealed preliminarily the sludge pyrolysis mechanisms. This fundamental study provides a basic insight into the sludge pyrolysis, which would benefit the efficient utilization of sewage sludge as an energy source.

1. Introduction

Sludge is the major byproduct of wastewater treatment plants worldwide. The management of sludge has become a problem of increasing urgency, involving substantial cost and effort. Sludge production has been increasing significantly in recent years due to more stringent regulation of wastewater treatment. For instance, sludge production in the United States was close to 6.9 million tons of dried solid (tds) in 1998 and estimated to increase to 7.1 in 2000, 7.6 in 2005, and 8.2 million tds in 2010.¹ It is expected that more than 8 million tds of sewage sludge will be generated in China by 2010.² In Singapore, around 80 000 tons of sewage sludge is generated each year from 6 wastewater reclamation plants (WRPs). Proper treatment of sludge is thus necessary to reduce the volume and to minimize the potential impacts of sewage sludge disposal.

At present, the most common disposal processes for sewage sludge include agriculture application, landfilling, and thermal conversion (combustion/incineration).^{3–5} However, the traditional disposal routes are coming under pressure, due to land

limitations and stringent regulations. It is necessary to develop a cost-effective and environmentally friendly solution. Lately, various modern technologies (e.g., pyrolysis, gasification, wet oxidation, etc.) have been introduced, providing an alternative trend to sewage sludge disposal, especially with the decreasing availability and the increasing price of land for landfilling.⁴

Pyrolysis is considered as a promising alternative technology that converts sludge to clean energy and valuable chemicals.³ It can also be optimized to maximize the production of gases, oils or chars, according to the specific applications.^{6–8} A higher yield of interest relies on a good understanding to the fundamentals and mechanisms of sludge pyrolysis. Nevertheless, sewage sludge is a heterogeneous material with a wide variety of inorganic and organic components, and the pyrolysis of sludge is a complicated process. It is therefore difficult to determine the sludge conversion pathways, since numerous thermal degradation reactions may occur simultaneously during the pyrolysis process.

To better understand the pyrolysis process of sewage sludge, many studies have been performed on the basis of thermogravimetric analysis (TGA) alone or combined with differential

[†] Presented at the International Conference on Bioenergy Outlook 2007, Singapore, April 26–27, 2007.

* To whom correspondence should be addressed. Telephone: 65-67943244. Fax: 65-67921291. E-mail: ryan@ntu.edu.sg.

[‡] Huazhong University of Science and Technology.

[§] Nanyang Technological University.

(1) USEPA. *Biosolids generation, use and disposal in the United States*; EPA530-R-99-009, U.S. EPA Office of Solid Waste: Washington, D.C. 1999; p 81.

(2) Cai, Q.-Y.; Mo, C.-H.; Wu, Q.-T.; Zeng, Q.-Y.; Katsoyiannis, A. *Chemosphere* **2007**, *68* (9), 1751–1762.

(3) Werther, J.; Ogada, T. *Prog. Energy Combust. Sci.* **1999**, *25* (1), 55–116.

(4) Fytli, D.; Zabaniotou, A. *Renew. Sust. Energ. Rev.* published online Aug 14, 2006, <http://dx.doi.org/10.1016/j.rser.2006.05.014>.

(5) Thipkhanthod, P.; Meeyoo, V.; Rangsunvigit, P.; Kitiyanan, B.; Siemanond, K.; Rirkosomboon, T. *Chemosphere* **2006**, *64* (6), 955–962.

(6) Piskorz, J.; Scott, D. S.; Westerberg, I. B. *Ind. Eng. Chem. Proc. Des. Dev.* **1986**, *25* (1), 265–270.

(7) Caballero, J. A.; Front, R.; Marcilla, A.; Conesa, J. A. *J. Anal. Appl. Pyrolysis* **1997**, *40–41*, 433–450.

(8) Inguanzo, M.; Dominguez, A.; Menendez, J. A.; Blanco, C. G.; Pis, J. J. *J. Anal. Appl. Pyrolysis* **2002**, *63* (1), 209–222.

scanning calorimetry (DSC)^{9–12} and bench-scale fluidized bed reactors.^{13–15} Recently, coupled techniques have been successfully used to characterize the gas- or liquid-phase compositions. The coupling of TGA and spectrometer techniques, such as Fourier transform infrared (FTIR) spectroscopy and mass spectrometry (MS), has been used on the pyrolysis of coal and biomass,^{16–20} and a few applications of this technique were found to deal with the pyrolysis of sewage sludge.^{21–24} Still, a literature survey shows no application of a gas production simulation which was done to assist the understanding of the mechanism of pyrolyzing sewage sludge.

In this study, a TGA-FTIR technique is applied to determine the pyrolysis characteristics of sewage sludge, and the results obtained are further utilized to calculate the kinetic parameters. The pyrolysis was carried out in a thermogravimetric reaction system at various heating rates and in a nitrogen atmosphere. A simple global reaction model was proposed to describe the pyrolysis of sewage sludge. The kinetic parameters were determined under the experimental conditions. The gas products released from the pyrolysis of sludge were analyzed online using an FTIR technique. The gas distribution was simulated using Outokumpu HSC Chemistry version 4.1. The objective of this study is to better understand the mechanism of sludge pyrolysis and provide a basic insight into sludge pyrolysis for optimum design of the pyrolysis system, which will benefit the efficient utilization of sewage sludge.

2. Experimental Section

2.1. Materials. Two sludge samples from two wastewater treatment plants were used. In these plants, different wastewater treatment operations and sludge processing were adopted, as listed in Table 1. Both samples were treated with seawater flushing, but with different treatment levels (primary or secondary) or dewatering processes; therefore, the chemical and physical properties of the two samples were diverse depending on the wastewater treatment process. To minimize the changes of sludge properties, they were dried at 105 ± 3 °C for 24 h to a constant weight to remove moisture prior to characterization. The sludge samples were then ground to pass through a $106 \mu\text{m}$ screen and stored in the desiccator before further analysis.

Proximate analysis of sludge samples was carried out by ASTM standard methods (D 5142-90) using a thermogravimetric analyzer (TGA, TA 2050, USA). Ultimate analysis was performed with a

Table 1. Treatment Processes Used for Sewage Sludge

sample ID	treatment level ^a	seawater flushing ^b	sludge dewatering process
S1	CEPT (using FeCl ₃ as coagulant) ^c	yes	centrifuge
S2	ST (activated sludge process)	yes	filter press

^a (ST) secondary treatment; (CEPT) chemically enhanced primary treatment. ^b Sewage would contain seawater, which has a high level of chloride ions, sulfate ions, and other mineral matters that may significantly affect the sludge characteristics. ^c FeCl₃ is dosed in the CEPT process as a coagulant.

CHNS/O elementary analyzer (PerkinElmer 2400II, USA). The calorific value of the studied samples was determined by bomb calorimeter (Parr 1266, Parr Instrument Company, USA) according to ASTM D 2015-91. The results are presented in Table 2. These showed that S1 had higher volatile matter and lower ash content than S2; therefore, the low heating value of S1 was much higher than that of S2, although S2 contained slightly higher C, H, and N content. If only the main elements (C, H, O) are considered, the molecular formula of the studied samples based on one C atom can be written as CH_xO_y, as given in the last column of Table 2.

Major elements in sludge ash samples (treated by low temperature ashing at 450 °C for about 15 h) were analyzed by X-ray fluorescence (XRF, Philips, PW2400, Netherlands), while trace elements were determined using inductively coupled plasma optical emission spectroscopy (ICP-OES, PerkinElmer, Optima 2000DV, USA). The results are summarized in Table 3. In relation to major and trace elements in the ashes, the sludge composition displayed heterogeneous properties due to different treatment methods used in the wastewater treatment process. Compared with results in the literature,²⁵ the sludge samples studied consisted of more S and Cl, which might attribute to seawater flushing. The contents of trace elements are also diverse in S1 and S2.

2.2. Apparatus and Methods. Pyrolysis of sludge samples was performed in a thermogravimetric analyzer (TGA, TA 2050, USA) under N₂ atmosphere. The sample size was maintained at 10 ± 1 mg with a particle size $< 106 \mu\text{m}$ for each run under nonisothermal conditions. The flow rate of balance gas and sample gas (pure N₂, 99.9995%) was kept both at 50 mL min^{-1} to ensure an inert atmosphere during the run. The sample was heated up from the ambient temperature to 105 °C and kept isothermal for approximately 5 min to ensure that free water was completely removed. Then, the sample was further heated to 900 °C at a preset heating rate varying between 5 and 20 °C min⁻¹. A slow heating rate was used to ensure that the heat transfer limitations could be ignored. To ensure the reproducibility and accuracy of analysis, repeated experiments were accomplished. For some cases, the test was repeated at least three times, and the average relative error over the whole weight loss curve was within $\pm 5\%$. Both the thermogravimetric (TG) and differential thermogravimetric (DTG) data were used to differentiate the pyrolysis behavior of two samples at different conditions as well as to provide the estimation of the kinetic parameters.

The gas products from the pyrolysis of sewage sludge in TGA (TA 2050, USA) were determined using a Fourier transform infrared spectrometer (Bio-Rad, USA). While other conditions were kept the same as those used in TGA, the sample size was controlled at ~ 20 mg to provide enough gas for analysis. To minimize the secondary reaction, the gas products released from thermogravimetric balance were swept immediately to a gas cell, followed by detection using the FTIR spectrometer equipped with a deuterated triglycine sulfate (DTGS) detector (Bio-Rad Excalibur Series, model FTS 3000). The transfer line and the head of the TG balance were heated at a constant temperature of 200 °C, to avoid the condensation of volatile decomposition products. The scanning range of IR was 4000–500 cm⁻¹, in terms of wavenumber. The resolution and

- (9) Urban, D. L.; Antal, J.; Michael, J. *Fuel* **1982**, *61* (9), 799–806.
 (10) Font, R.; Fullana, A.; Conesa, J. A.; Llavador, F. *J. Anal. Appl. Pyrolysis* **2001**, *58–59*, 927–941.
 (11) Chen, X.; Jeyaseelan, S. *J. Environ. Eng.* **2001**, *127* (7), 585–593.
 (12) Stolarek, P.; Ledakowicz, S. *Water Sci. Technol.* **2001**, *44* (10), 333–339.
 (13) Stambach, M. R.; Kraaz, B.; Hagenbucher, R.; Richarz, W. *Energy Fuels* **1989**, *3* (2), 255–259.
 (14) Duempelmann, R.; Richarz, W.; Stambach, M. R. *Can. J. Chem. Eng.* **1991**, *69* (4), 953–963.
 (15) Shen, L.; Zhang, D. K. *Fuel* **2003**, *82* (4), 465–472.
 (16) Bassilakis, R.; Carangelo, R. M.; Wojtowicz, M. A. *Fuel* **2001**, *80* (12), 1765–1786.
 (17) Arenillas, A.; Pevida, C.; Rubiera, F.; Garcia, R.; Pis, J. J. *J. Anal. Appl. Pyrolysis* **2004**, *71* (2), 747–763.
 (18) Yang, H.; Yan, R.; Chin, T.; Liang, D. T.; Chen, H.; Zheng, C. *Energy Fuels* **2004**, *18* (6), 1814–1821.
 (19) Yang, H.; Yan, R.; Chen, H.; Lee, D. H.; Liang, D. T.; Zheng, C. *Energy Fuels* **2006**, *20* (3), 1321–1328.
 (20) Fang, M. X.; Shen, D. K.; Li, Y. X.; Yu, C. J.; Luo, Z. Y.; Cen, K. F. *J. Anal. Appl. Pyrolysis* **2006**, *77* (1), 22–27.
 (21) Conesa, J. A.; Marcilla, A.; Moral, R.; Moreno-Caselles, J.; Perez-Espinoza, A. *Thermochim. Acta* **1998**, *313* (1), 63–73.
 (22) Chen, X.; Jeyaseelan, S. *J. Environ. Eng.* **2001**, *127* (7), 585–593.
 (23) Otero, M.; Diez, C.; Calvo, L. F.; Garcia, A. I.; Moran, A. *Biomass Bioenergy* **2002**, *22* (4), 319–329.
 (24) Karayildirim, T.; Yanik, J.; Yuksel, M.; Bockhorn, H. *Fuel* **2006**, *85* (10–11), 1498–1508.
 (25) Font, R.; Fullana, A.; Conesa, J. J. *J. Anal. Appl. Pyrolysis* **2005**, *74* (1–2), 429–438.

Table 2. Proximate and Ultimate Analyses of Sewage Sludge Samples

	proximate analysis (wt %) ^a				ultimate analysis (wt %, dry basis)					LHV (MJ/kg) ^c	molecular formula
	M _{ar}	V _d	A _d	FC _d	C	H	N	S	O ^b		
S1	64.11	75.25	23.41	1.34	33.00	4.35	2.02	0.5	36.72	25.63	CH _{1.58} O _{0.83}
S2	77.66	66.20	26.76	7.04	38.09	8.94	5.91	2.03	18.27	19.87	CH _{2.82} O _{0.35}

^a M, moisture content; V, volatile matters; A, ash; FC, fixed carbon; ar, on as-received basis; d, on dry basis. ^b Determined by difference. ^c Low heating value.

Table 3. Ash Characterization of Sewage Sludge Samples

sample	major elements weight percentage in ash (wt %)										
	SiO ₂	Al ₂ O ₃	CaO	MgO	K ₂ O	Na ₂ O	Fe ₂ O ₃	TiO ₂	P ₂ O ₅	SO ₃	Cl
S1	13.04	13.23	13.45	3.71	2.54	6.09	20.41	0.51	10.45	12.63	3.92
S2	5.55	7.34	8.31	3.61	1.25	6.22	35.11	0.54	15.74	15.10	1.23

sample	trace elements weight content in ash (μg/g)									
	Co	Mn	Ni	V	Zn	Cu	Cr	Pb	Cd	
S1	30	347	194	94	2190	1960	524	145	5	
S2	52	520	300	73	3040	6280	214	159	5	

sensitivity were set at 4 cm⁻¹ and 1, respectively. FTIR spectra of the gas products were collected continuously with the baseline corrected.

2.3. Calculation of Kinetic Parameters. A kinetic study of sewage sludge pyrolysis is necessary to achieve an efficient production of fuel gases, chemicals, and energy. The information is also important for the design of large-scale pyrolysis reactors. In this study, it was assumed that the pyrolysis of sludge was controlled mainly by chemical decomposition as the gas-phase and internal mass and heat transfer limitation could be negligible at the conditions selected. The kinetic parameters (activation energy and reaction order) could be calculated, based on the following principles.

The pyrolysis of sewage sludge is assumed to be the following:



The global reaction kinetics of sewage sludge pyrolysis can be described by the following rate equation:²⁶

$$\frac{dX}{dt} = k(1 - X)^n \quad (1)$$

where X is thermal conversion of sewage sludge at time t and is given as $X = (W_i - W)/(W_i - W_f)$, where W_i , W , and W_f refer to the initial, present, and final residual amounts, respectively, and n is the order of reaction. Constant k obeys Arrhenius equation

$$k = A \exp\left(-\frac{E}{RT}\right) \quad (2)$$

where the kinetic parameters E and A represent the activation energy and the pre-exponential factor of the reaction, respectively; R is the universal gas constant; and T is the absolute temperature.

For a constant heating rate of $\beta = dT/dt$, eqs 1 and 2 were combined as

$$\frac{dX}{dT} = \left(\frac{1}{\beta}\right) A \exp\left(-\frac{E}{RT}\right) (1 - X)^n \quad (3)$$

According to our experimental conditions, the nonisothermal method (i.e., where the sample was heated at a selected heating rate) was used; therefore, a rearranged and integral form of eq 3 is normally written as

$$G(X) = \int_{T_0}^T \left(\frac{A}{\beta}\right) \exp\left(-\frac{E}{RT}\right) dT \quad (4)$$

where $G(X) = \int_0^X [dX/(1 - X)^n]$. Following the Coats and Redfern approximation method,^{5,26} eq 4 becomes

$$\ln\left[\frac{G(X)}{T^2}\right] = \ln\left[\frac{AR}{\beta E}\right] \left[1 - \frac{2RT}{E}\right] - \frac{E}{RT} \quad (5)$$

Usually, for most temperatures and activation energies, $RT/E \ll 1$, and $1 - 2RT/E \approx 1$; therefore, the kinetic mechanism equation can be simplified as

$$\ln\left[\frac{G(X)}{T^2}\right] = \ln\left[\frac{AR}{\beta E}\right] - \frac{E}{RT} \quad (6)$$

$$G(X) = -\ln(1 - X) \quad (\text{for } n = 1) \quad (7)$$

$$G(X) = \frac{1 - (1 - X)^{1-n}}{1 - n} \quad (\text{for } n \neq 1) \quad (8)$$

If the reaction order is appropriate, the plot of $\ln(G(X)/T^2)$ versus $1/T$ should be a straight line; thus, the activation energy E can be obtained from the slope, and the pre-exponential factor A can be obtained from the intercept.

2.4. Simulation of Gas Components. The HSC Chemistry version 4.1 software (Outokumpu, Finland)²⁷ was used for calculations of gas products from sludge pyrolysis. Details on the simulation method can be found in our previous study.²⁸ HSC calculation is based on the assumption of minimizing the total Gibbs free energy of the system in the equilibrium state. The thermodynamic calculation was preformed with C, H, and O bearing species in sludge for simplification. Only S1 was considered as representative; its normalized molecular formula is CH_{1.58}O_{0.83} as given in Table 2 which was used as input for the HSC calculation. About 46 species were included in the calculation system, which were listed in Table 4.

3. Results and Discussion

3.1. Thermal Conversion Behaviors. Thermogravimetric analysis provides prior knowledge of pyrolysis behavior of sewage sludge under the inert atmosphere.²⁴ Studies on TG profiles contribute to enhancing the knowledge of the kinetics of this thermal process and, therefore, to establishing the optimum operational conditions for better utilization of sewage sludge.

A series of experiments were systematically carried out by means of TGA at 5, 10 and 20 °C min⁻¹ heating rates, respectively. The mass loss and the rate of mass loss during pyrolysis of two sewage sludge samples are shown in Figure 1.

(27) Roine, A., *Outokumpu HSC chemistry for windows: chemical reaction and equilibrium software with extensive thermochemical database*; Outokumpu Research: Oy, Finland, June, 1999.

(28) Lee, D. H.; Yang, H.; Yan, R.; Liang, D. T. *Fuel* **2007**, *86* (3), 410-417.

Table 4. Species Considered in the HSC Calculation

C-bearing species	H-bearing species	O-bearing species
C, C(g), C(H ₃)(g), C ₂ (g), C ₂ H(g), C ₂ H ₂ (g), C ₂ H ₃ (g), C ₂ H ₄ (g), C ₂ H ₅ (g), C ₂ H ₆ (g), C ₂ O(g), C ₃ (g), C ₃ O ₂ (g), C ₄ (g), C ₅ (g), CH(g), CH ₂ (g), CH ₃ (g), CH ₄ (g), CO(g), CO ₂ (g), COOH(g), HCO(g), HCOOH(g)	C ₂ H(g), C ₂ H ₂ (g), C ₂ H ₃ (g), C ₂ H ₄ (g), C ₂ H ₅ (g), C ₂ H ₆ (g), CH(g), CH ₂ (g), CH ₃ (g), CH ₄ (g), COOH(g), H(g), H ₂ (g), H ₂ O(g), H ₂ O ₂ (g), HCO(g), HCOOH(g), HO(g), HO ₂ (g)	(H ₃)O ₂ (g), C ₂ O(g), C ₃ O ₂ (g), CO(g), CO ₂ (g), COOH(g), H ₂ O, H ₂ O(g), H ₂ O ₂ (g), HCO(g), HCOOH(g), HO(g), HO ₂ (g), O(g), O ₂ (g), O ₃ (g)

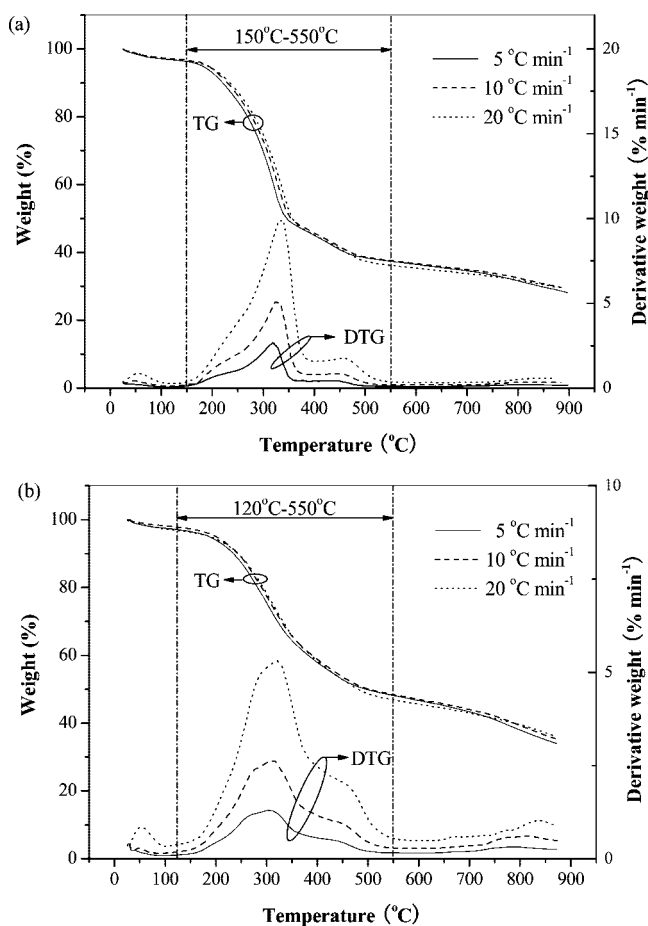


Figure 1. Pyrolysis characteristics of Sewage sludge: (a) S1, (b) S2.

Table 5. Pyrolysis Parameters of Sewage Sludge from Thermogravimetric Data

sample ID	heating rate (°C min ⁻¹)	peak temperature (°C)	corresponding peak height (% min ⁻¹)	final residues (wt %)
S1	5	319 ± 4, 440 ± 3	2.67, 0.43	28.1
	10	324 ± 1, 450 ± 2	5.06, 0.85	29.63
	20	340 ± 2, 459 ± 3	9.91, 1.77	29.82
S2	5	302 ± 2	1.29	31.74
	10	308 ± 1	2.62	32.69
	20	320 ± 3	5.32	34.52

It was found that the decomposition of S1 mainly occurred in the temperature range from 150 to 550 °C. The first decomposition stage happened between 150 and 380 °C, which was most likely related to the depolymerization reactions, while the second stage was located at approximately 380–550 °C, as a consequence of the further degradation of volatile matters. A slight weight loss was also observed at temperatures above 550 °C, where a complete decomposition occurred. The residues of S1

after the running at 5, 10, and 20 °C min⁻¹, were 28.1, 29.63, and 29.82 wt %, respectively. The temperature ranges for S1 decomposition were slightly different from those reported by Chen and Jeyaseelan,²² where the depolymerization and secondary

degradation occurred at 174–325 and 325–455 °C, respectively. This might be attributed to the heterogeneity of the sludge samples.

For S2 sludge, one obvious peak was found in the DTG curves in the temperature range of 120–550 °C, shown in Figure 1b. It was attributed to the abundant release of volatile matter in S2. The main decomposition or pyrolysis stage started slowly after dehydration and increased sharply after 200 °C. It reached the peak at about 300–320 °C according to different heating rates and then ceased at ~550 °C. The remaining weights for S2 pyrolysis were 31.74, 32.69, and 34.52 wt % after running at 5, 10, and 20 °C min⁻¹, respectively, which was higher than the values of S1, due to possibly the higher ash contents occurring in S2 (see Table 2). The overall decomposition of S2 was governed by one single stage, although a slight “shoulder peak” was observed at high heating rates (10 and 20 °C min⁻¹). This result was in a good agreement with that of Thipkhunthod et al.,⁵ who reported that the pyrolysis of one major type of sludge occurred mainly after 200 °C and ceased at 550 °C and that one DTG peak was found at 299 °C.

The heating rate is one of the most important parameters influencing the thermal decomposition characteristics. Figure 1 and Table 5 showed that a higher heating rate led to increase of the maximum devolatilization rate and the temperature corresponding to the peak. For example, the maximum degradation temperature was 319, 324, and 340 °C for the first step of S1 at heating rates of 5, 10, and 20 °C min⁻¹, with the corresponding peak height or reaction rate of about 2.67, 5.06, and 9.91% min⁻¹, respectively. Similarly for S2, a peak was found at 302, 308, and 320 °C, with the reaction rate of 1.29, 2.62, and 5.32% min⁻¹, respectively, at different heating rates. This shift of peak towards a higher temperature, with an increasing heating rate, was possibly caused by the effect of the kinetics of the decomposition, which resulted in a delayed degradation. This observation was consistent with that of Shie et al.,²⁹ who reported that a higher heating rate resulted in a higher peak value of reaction rate and a higher temperature for its occurrence.

The curves of sludge conversion versus temperature (at a heating rate of 10 °C min⁻¹) in pyrolysis are shown in Figure 2. The pyrolysis of S1 was obviously divided into two parts, while the pyrolysis of S2 only consisted of one main stage. It was consistent with the earlier findings: two maximum decomposition rates of S1 were found in Figure 1a while one was observed for S2 in Figure 1b. These results suggested that the pyrolysis of S1 would proceed following a two-stage reaction while S2 would proceed in one stage. The different sources of the two sludge samples and thus their diverse chemical and physical natures differentiated their characteristics of pyrolysis. In previous reports, several decomposition stages were also identified in sludge pyrolysis. Font et al.²⁵ found that the experimental decomposition was not satisfactorily correlated considering only one fraction and at least two or three fractions must be considered. Urban and Antal⁹ proposed two independent reactions associated with the decomposition of dead bacteria

(29) Shie, J. L.; Chang, C. Y.; Lin, J. P.; Wu, C. H.; Lee, D. J. *J. Chem. Technol. Biotechnol.* **2000**, *75* (6), 443–450.

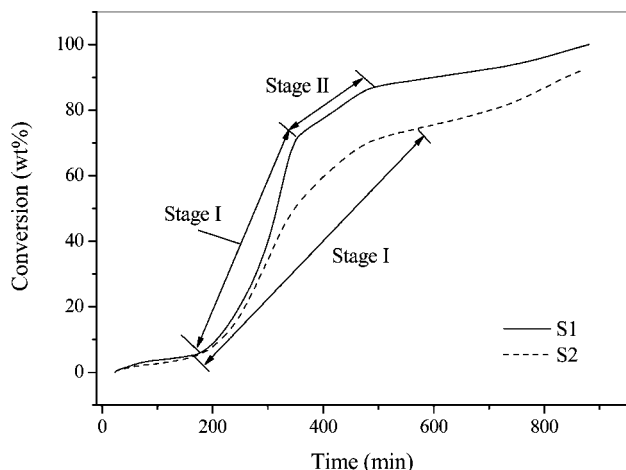


Figure 2. Curves of conversion versus temperature (at a heating rate of $10\text{ }^{\circ}\text{C min}^{-1}$) for S1 and S2.

and settled organics, whereas Conesa et al.³⁰ suggested a scheme considering three independent stages, corresponding to biodegradable matter, dead bacteria, and nonbiodegradable matter, respectively.

In the present study, differences of pyrolysis stages between two sludge samples might come from the different contents of biodegradable matter, dead bacteria, and nonbiodegradable matter associated, due to the different sources of the operations applied in the wastewater treatment plant (see Table 1). For S1, stage I might be related to the decomposition of biodegradable matter, which accounted for about 70% of the total weight loss (see Figure 1a), while stage II was possibly corresponding to the degradation of dead bacteria possessing 17% of weight loss. The remaining 13% of total weight loss may have resulted from the nonbiodegradable matter occurring only at higher temperatures ($>550\text{ }^{\circ}\text{C}$). Similarly for S2, only one obvious reaction was observed, which accounted for 70% of total weight loss ($<550\text{ }^{\circ}\text{C}$), possibly owing to the joint degradation of biodegradable matter and dead bacteria. The remaining weight loss occurred at a much higher temperature ($>550\text{ }^{\circ}\text{C}$), attributed to the decomposition of nonbiodegradable matter, which was very hard to degrade at lower temperatures. Nevertheless, the components of sludge need to be verified using biological methods to further support this postulation.

3.2. Kinetic Parameters. The reaction scheme of sewage sludge pyrolysis is very complex. Determining the kinetic parameters is of importance for enhancing awareness of the reaction. Many models have been proposed for pyrolysis of sludge in prior studies.^{9,22,25,30,31} The decomposition of sludge could be described with one or more reaction models, due to the varieties of sewage sludge. In the present research, the global reaction kinetic model was considered, with the detailed principles described previously.

To best fit the experiment results, different reaction orders (ranging from 0 to 10) were assumed and the kinetic parameters were calculated using eqs 6–8. The obtained kinetic parameters including the activation energy, pre-exponential factor, and reaction order are summarized in Table 6. It can be seen that the activation energies of S1 for the first reaction stage were close to those of S2, at $\sim 30\text{ kJ mol}^{-1}$, regardless of the heating rates used. The relatively lower activation energies obtained here might be attributed to the effect of heat transfer on the samples

studied. In addition, the activation energies of S1 in the first reaction were more than double those in the second reaction, which showed that the main decomposition of S1 occurred in the first step in the temperature range $150\text{--}380\text{ }^{\circ}\text{C}$. The pre-exponential factors increased with the heating rate. The orders of all reactions were found in the range of 1–2, which were best fit to the pyrolysis of the studied sewage sludge, with the correlation coefficients (R) all at ~ 0.99 . The activation energy in the range of $17\text{--}332\text{ kJ mol}^{-1}$ for sludge pyrolysis has previously been reported.³⁰ Though the values of kinetic parameters may not be comparable, due to the difference of samples analyzed and models used, the activation energy of the studied samples was in agreement with those reported in the literature.^{22,30} The reaction orders presented in this study were in line with that of Thipkhunthod et al.⁵ and were reasonable for most chemical reactions.

3.3. TG-FTIR Analysis of Gas Products. Thermogravimetric analysis has proven to be a very useful technique for studying the pyrolysis of a wide range of solid samples. However, TG analysis itself does not identify the decomposition products. FTIR is currently one of the most powerful techniques for gas analysis. Therefore, TG coupled with FTIR was used in this study to measure weight loss and evolution of volatiles for S1 at the heating rate of $10\text{ }^{\circ}\text{C min}^{-1}$. The volatiles determined with TG-FTIR analysis were CH_4 , C_2H_4 , CO , CO_2 , H_2O , and some organics. An FTIR stack plot of S1 in the temperature range of $200\text{--}600\text{ }^{\circ}\text{C}$ for one trial is shown in Figure 3 where the temperature is referring to that in TGA. A typical spectrum of S1 subtracted from Figure 3 at $350\text{ }^{\circ}\text{C}$ is also given in Figure 4 for a better and clearer display, which both demonstrated the characteristic wave numbers of gas species, including CH_4 ($3025\text{--}3000\text{ cm}^{-1}$), CO_2 ($2400\text{--}2250\text{ cm}^{-1}$), CO ($2250\text{--}2200\text{ cm}^{-1}$), and aldehydes and acids ($1660\text{--}1820\text{ cm}^{-1}$).

It can be observed from Figure 3 that, at low temperature ($200\text{ }^{\circ}\text{C}$), only a small absorbance band of CO_2 was observed on the spectrum. Nevertheless, the absorbance bands of water (at $3700\text{--}3550\text{ cm}^{-1}$ and $1550\text{--}1350\text{ cm}^{-1}$) were not obvious, although they were speculated to be there due to the dehydration of the sludge by losing both free water and chemically bonded water, previously evidenced by TGA analysis. This might account for the wide absorption bands of water in the FTIR spectrum. At temperatures of $200\text{--}350\text{ }^{\circ}\text{C}$, the release of CO_2 increased significantly and reached the maximum yield at about $350\text{ }^{\circ}\text{C}$, which should be corresponding to the peak of the weight loss rate in the DTG curve (see Figure 1a) occurring at $324\text{ }^{\circ}\text{C}$. The slight temperature difference was attributed to the time lapse of gas passing through the TGA-FTIR interface. Meanwhile, another obvious peak of CO appeared from $350\text{ }^{\circ}\text{C}$, coming from the incomplete oxidation of combustible carbon in sludge. At temperatures $>350\text{ }^{\circ}\text{C}$, the release of CO_2 and CO decreased as the temperature increased further, possibly indicating the completion of stage I pyrolysis (see Figure 1a). After that, the release of CH_4 was increased and reached its maximum at about $550\text{ }^{\circ}\text{C}$. In addition, some peaks were found in the wave number range of $1660\text{--}1820\text{ cm}^{-1}$ at temperatures above $350\text{ }^{\circ}\text{C}$, which were associated with carbonyl bond compounds, including acids, esters, aldehydes, and ketones. These organics were intermediate fragments in sludge pyrolysis, and since they appeared only at high temperatures, they were most likely related to the second stage of S1 pyrolysis, in which secondary degradation of volatile matters occurred. The decomposition of these organics at higher temperature led to the further releasing of CO_2 in gas products.

(30) Conesa, J. A.; Marcilla, A.; Prats, D.; Rodriguez-Pastor, M. *Waste Manage. Res.* **1997**, *15* (3), 293–305.

(31) Scott, S. A.; Dennis, J. S.; Davidson, J. F.; Hayhurst, A. N. *Fuel* **2006**, *85* (9), 1248–1253.

Table 6. Kinetic Parameters for the Pyrolysis of Sewage Sludge^a

		reaction I				reaction II			
		<i>E</i> (kJ mol ⁻¹)	<i>A</i> (min ⁻¹)	<i>n</i>	- <i>R</i> ^b	<i>E</i> (kJ mol ⁻¹)	<i>A</i> (min ⁻¹)	<i>n</i>	- <i>R</i>
S1	5 °C min ⁻¹	31.87	27.35	1.1	0.9823	12.96	0.52	1.9	0.9921
	10 °C min ⁻¹	32.84	59.73	1	0.9962	15.41	1.99	1.9	0.9912
	20 °C min ⁻¹	30.92	67.82	1	0.9918	18.62	8.97	1.9	0.9891
S2	5 °C min ⁻¹	29.81	15.15	2	0.9959				
	10 °C min ⁻¹	31.75	44.47	1.9	0.9965				
	20 °C min ⁻¹	30.25	63.75	1.9	0.9921				

^a *E*, activation energy; *A*, pre-exponential factor; *n*, reaction order. ^b *R*, correlation coefficient.

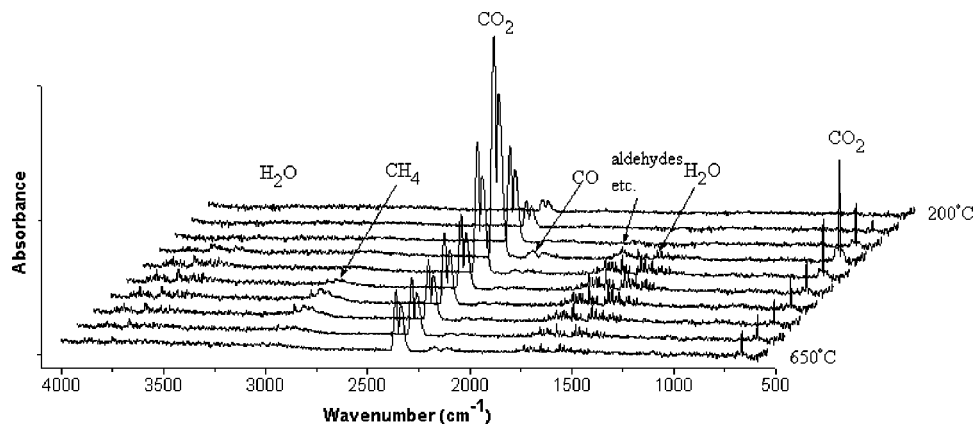


Figure 3. FTIR stack plot of the gas products from pyrolysis of S1 (heating rate 10 °C min⁻¹).

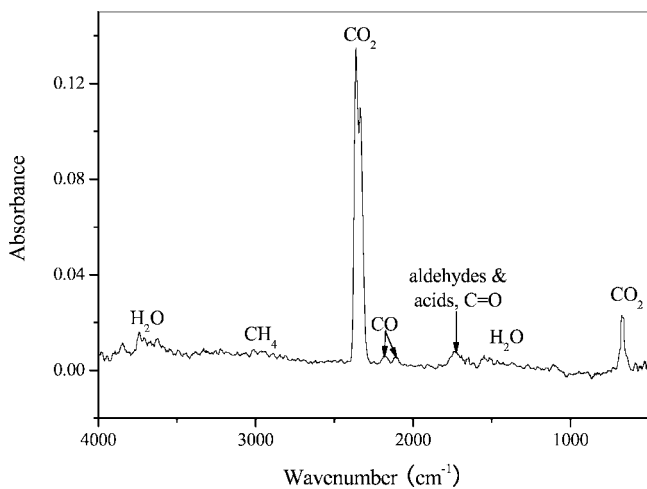


Figure 4. FTIR spectra of sludge S1 at 350 °C with the heating rate of 10 °C min⁻¹.

Some of the gaseous products, such as H₂, H₂S, N₂, and polyaromatic hydrocarbons, cannot be detected with the FTIR technique, due to either low sensitivity or weak absorption. However, this method provides a rapid online analysis of gas products within seconds, which facilitates our research on the kinetics and gaseous species evolution. It is recommended that other devices, such as Micro-GC, GC-MS, and TG-MS, could be further used to obtain more complete information to better understand the gas distribution from sludge pyrolysis.

3.4. Simulation of Gas Composition. The decomposition of sewage sludge can be simplified as “sludge → H₂ + CO +

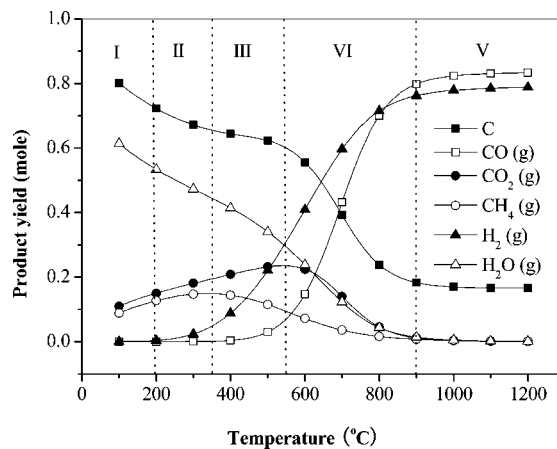


Figure 5. Gas distribution of sludge pyrolysis calculated with HSC software

CO₂ + hydrocarbon + charcoal”, in which charcoal remained as a solid at temperatures above 900 °C. The representative expression for the HSC calculation in the present study was obtained as CH_{1.58}O_{0.83} for S1 as shown in Table 2. The results from the calculation based on 1 mol of C atoms in the expression as input in HSC are plotted in Figure 5. It indicated that content of carbon (C) decreased with increasing temperature and became almost constant at 0.17 when the temperature was above 900 °C, implying the existence of charcoal remaining in the solid when the temperature increased further.

Five distinct regions of temperature were seen in Figure 5 for pyrolysis gas distribution, i.e., *T* < 200 °C, 200 < *T* < 350 °C, 350 < *T* < 550 °C, 550 < *T* < 900 °C, and *T* > 900 °C,

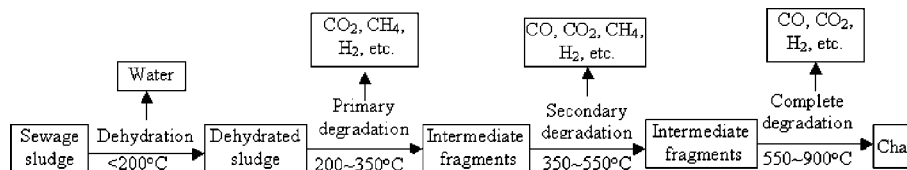


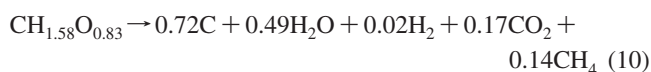
Figure 6. Schematic of pyrolysis mechanism of sewage sludge.

as marked from I to V. Therefore, the following equations were proposed for sludge pyrolysis, based on the major products predicted by HSC (see Figure 5). The coefficient for each product shown in the equations was obtained from the average value in each region.

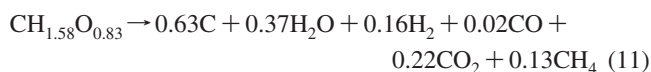
I. For $T < 200$ °C:



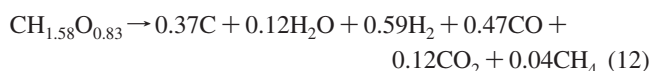
II. For $200 < T < 350$ °C:



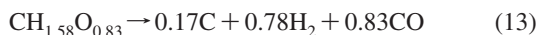
III. For $350 < T < 550$ °C:



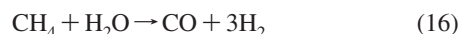
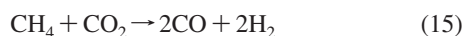
IV. For $550 < T < 900$ °C:



V. For $T > 900$ °C:



Region I ($T < 200$ °C) represented the dehydration process, where free water and some light organics such as CO_2 and CH_4 were released. The predicted CO_2 release at low temperature was consistent with the results shown in FTIR spectrum (see Figure 3). In region II ($200 < T < 350$ °C), the major decomposition or depolymerization occurred, which was accompanied by the decrease of carbon and water and the increase of CO_2 and CH_4 in the products. The content of CH_4 reached maximum value at 350 °C. Meanwhile a very small amount of H_2 was given off. It can be seen from the TG curves (see Figure 1) that about 70% weight loss of the total was obtained the same temperature range ($200 < T < 350$ °C), indicating that the primary pyrolysis reaction of biodegradable sludge occurred in this region. The increasing release of CO_2 and CH_4 (as predicted) with temperature was also consistent with the observations from FTIR, whereas the corresponding temperatures at their maximum releases in prediction and FTIR experiment were different. In region III ($350 < T < 550$ °C), the second decomposition happened. The contents of combustible carbon, water vapor and methane, decreased further, while the contents of H_2 , CO , and CO_2 continually increased in this region. In region IV ($550 < T < 900$ °C), the contents of H_2 and CO increased significantly with the decrease of other species. In TGA, approximately 13% weight loss of the total was gained in this temperature range (Figure 1), which might be caused by the decomposition of nonbiodegradable or resulted from the following reductive reactions:



In the last region, pyrolysis of sludge was to complete, and almost no more reactions occurred. The contents of H_2 and CO were kept high and stable, while carbon residue remained constant, due to the formation of charcoal from carbonization.

Although some prediction results were in good agreement with the experimental data from TGA and FTIR analyses, such as the release of CO_2 , discrepancies were still found. For

example, in the FTIR spectrum, CH_4 was observed to release originally at high temperature (above 350 °C) and reach the maximum at about 500 °C, while in simulation most of CH_4 was produced at temperatures lower than 650 °C and reached the maximum at 350 °C. In addition, a large amount of constant CO and H_2 were found at high temperature from HSC calculation, while a decreasing CO peak was observed in the FTIR spectrum with increasing temperature. These discrepancies were attributed to the simple assumption that only thermodynamics was considered in simulation, whereas the kinetic and mass transfer constrains were ignored. Therefore, the thermodynamic simulation results might not be the same as those found in real situations, due to the limitations of thermodynamic calculations and the big differences between an experiment in a TGA (an open system) and the calculations (for a closed system). A better simulation could be achieved with considering both thermodynamic and kinetics in sludge pyrolysis in future studies.

In order to gain an overall viewpoint, the pyrolysis mechanism of sludge (S1) was illustrated in Figure 6 corresponding to the five temperature regions mentioned above. It indicated the sludge pyrolysis pathways in terms of gas releasing and changing of solid sludge via dehydration, formation of intermediates, decomposition of intermediates, and finally char generation, with increasing temperature. The releasing of hydrogen (H_2) was unfortunately not detected, due to the limitation of FTIR, which was predicted in the simulation results and also confirmed in other experimental work.⁵

4. Conclusions

Two sewage sludge samples were pyrolyzed in TGA, and their pyrolysis characteristics, kinetic parameters, and gas product distribution were investigated through experimental study and HSC simulation. The mechanisms of sludge pyrolysis were elucidated in depth. The following conclusions can be drawn out:

(1) Pyrolysis characteristics: the pyrolysis of sludge in TGA mainly occurred at temperatures lower than 550 °C. The maximum devolatilization rate and the temperature corresponding to it were increased with the increasing of heating rate. Two sludge samples demonstrated different pyrolysis characteristics—one contained two stages while another only one stage—due to most likely their different natures and sources from wastewater treatment processes.

(2) Kinetics: the activation energies, pre-exponential factors, and reaction orders were determined for both samples in pyrolysis. The activation energies were similar for two samples studied in the first stage, regardless the heating rate used. In contrast, the pre-exponential factors were found to increase with the heating rate. The kinetic parameters calculated explained well the pyrolysis characteristics observed.

(3) Gas products: the pyrolysis gas comprised mainly of CO , CO_2 , CH_4 , and light hydrocarbons in FTIR analysis. The releasing of these gas species was consistent with the weight loss of sludge in pyrolysis. In addition, the gas product distribution versus temperature was predicted using HSC, which indicated the large existence of hydrogen, although FTIR was incapable of detecting it.

(4) Mechanism: a further analysis by dividing the whole pyrolysis of sludge into five temperature regions revealed the sludge pyrolysis mechanisms. A series of reactions were proposed to assist a better understanding to the sludge pyrolysis pathways. The pyrolysis characteristics and kinetic parameters

obtained from TGA and gas releasing properties observed from FTIR were in a good agreement, and they were jointly supportive to the suggested mechanisms, although certain discrepancies between experiment and simulation existed in terms of gas releasing. A better understanding to the overall process of sludge pyrolysis was attained based on the complete fundamental study.

Acknowledgments. This research is supported by the National Natural Science Foundation of China (Grant No. 50676037). This work is also part of the project “Co-control of Pollutants during Solid Fuel Utilization”, supported by the Programme of Introducing Talents of Discipline to Universities (project B06019), China.

EF700287P